

Supporting Information

**Study on a polyacrylate-based waterborne coating: facile preparation, convenient self-healing behavior and photoluminescent property**

Bo Wu<sup>a</sup>, Anqian Yuan<sup>a</sup>, Yao Xiao<sup>b</sup>, Yi Wang<sup>a</sup> and Jingxin Lei<sup>a,\*</sup>

<sup>a</sup> State key laboratory of Polymer Materials Engineering, Polymer Research Institute of Sichuan University, Chengdu 610065, China

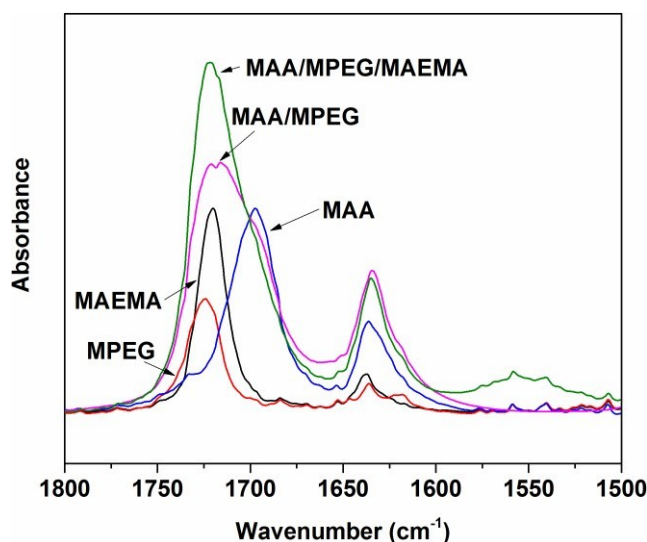
<sup>b</sup> College of Chemistry and Chemical Engineering, China West Normal University, Nanchong 637002, China

Corresponding Author

\* E-mail: [jxlei@scu.edu.cn](mailto:jxlei@scu.edu.cn). Tel: +86-0288540115

**Table S1** The recipes of WPACs samples.

Samples	MAA	MAEMA	MPEG	Mass ratio of MPEG	Molar ratio of MAA to MAEMA
WPAC-1:0	25.8 g	0 g	38.7 g	60 wt%	1:0
WPAC-3:1	25.8 g	15.7 g	62.3 g	60 wt%	3:1
WPAC-2:1	25.8 g	23.6 g	74.1 g	60 wt%	2:1
WPAC-1:1	25.8 g	47.1 g	109.4 g	60 wt%	1:1

**Fig. S1** FTIR spectra of monomers and their mixtures.

The FTIR spectra of MAA, MAEMA and MPEG as well as their mixtures are shown in Fig. S1. In MPEG's spectrum, the absorption peak at around  $1718\text{ cm}^{-1}$  is resulted from the free  $\text{-C=O}$  groups of ester bonds, which is also detected in the spectrum of MAEMA. In the spectrum of MAA/MPEG mixtures, there is a broad absorption between  $1750\text{ cm}^{-1}$  and  $1670\text{ cm}^{-1}$  corresponding to different states of carboxyl groups. The lower absorption centered at  $1722\text{ cm}^{-1}$  should be attributed to the stretching vibration of free carboxyl groups, the middle absorption peaks at around  $1716\text{ cm}^{-1}$  is ascribed to the H-bonded carboxyl stretching vibration (H bonds between MPEG and MAA), and the higher absorption peak at around  $1697\text{ cm}^{-1}$  is resulted from the MAA dimers (H bonds between MAA). In the spectrum of ternary MAA/MAEMA/MPEG mixtures, there is also a broad absorption band in a wavenumber range of  $1670\text{--}1670\text{ cm}^{-1}$ , further confirming the co-existence of two kinds of H bonds. In addition, a characteristic peak at around  $1558\text{ cm}^{-1}$  was observed, which is derived from the stretching vibration of ionized carboxyl groups, indicative of the existence of ionic bonds between MAA and MAEMA. Meanwhile, the obvious peaks at around  $1636\text{ cm}^{-1}$  should be ascribed to the stretching vibration of  $\text{C=C}$  groups.

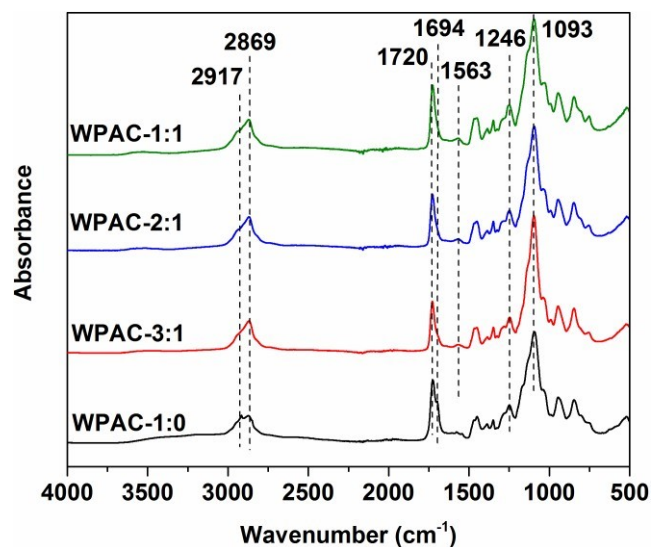


**Fig. S2** FTIR spectra of WPACs.

The FTIR characterization was conducted to reveal the chemical structure of WPACs. As shown in Fig. S2, there is no absorption at around  $1635\text{ cm}^{-1}$  (stretching vibration of  $\text{C}=\text{C}$ ), suggesting that the monomers were totally polymerized during copolymerization processes. In the spectrum of WPAC-1:0, the obvious peaks in the range of  $1750\text{--}1675\text{ cm}^{-1}$  should be ascribed to the stretching vibration of free carboxyl groups and H-bonded carboxyl groups. As for WPAC-3:1, WPAC-2:1 and WPAC-1:1, the similar absorption peaks are also observed at around  $1700\text{ cm}^{-1}$ , while the newly appeared peak at around  $1562\text{ cm}^{-1}$  should be assigned to the antisymmetric stretching vibration of ionized carboxyl groups, which is resulted from the interaction between carboxyl groups and tertiary amine groups, confirming the existence of H bonds and ionic bonds in polymer network. Meanwhile, characteristic peaks at around  $2940\text{ cm}^{-1}$ ,  $2869\text{ cm}^{-1}$ ,  $1451\text{ cm}^{-1}$ ,  $1095\text{ cm}^{-1}$  corresponding to methyl, methylene, ester bond, ether bond are also detected.

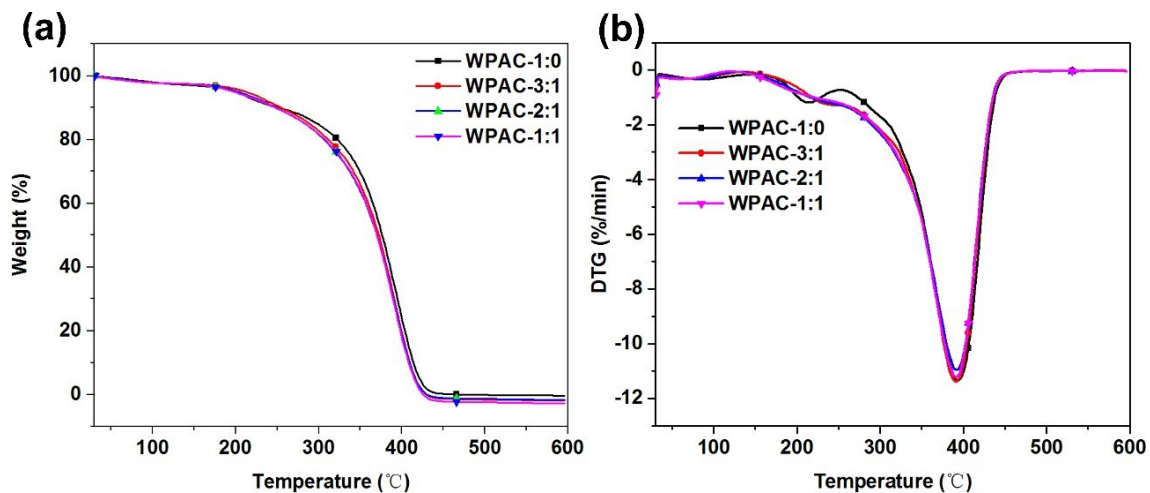


**Fig. S3** (a) TG and (b) DTG curves of WPAC-1:0, WPAC-3:1, WPAC-2:1 and WPAC-1:1.

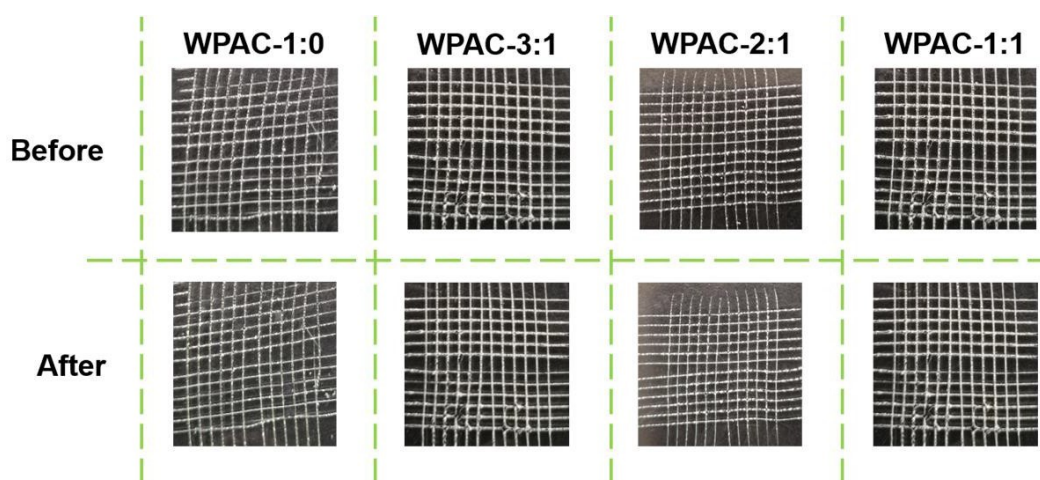


**Fig. S4** Photographs of scratched coatings before and after a pressure-sensitive tape was pulled off from the coating surface in the tape-and-peel test.

The adhesive force of the prepared WPACs coatings on glass substrate were measured by using the tape-and-peel test. In detail, the coatings were cut to obtain more than one hundred square lattice. The notches of WPACs coatings reach deep into the surface of glass substrate. Next, a pressure-sensitive tape was applied to the coating surface and then pulled off to determine the coating adhesion force. As can be seen from Fig. S4, there is almost no change of the coatings surface before and after the tape was pulled off, indicative of the robust adhesion of our prepared coatings on glass substrate.

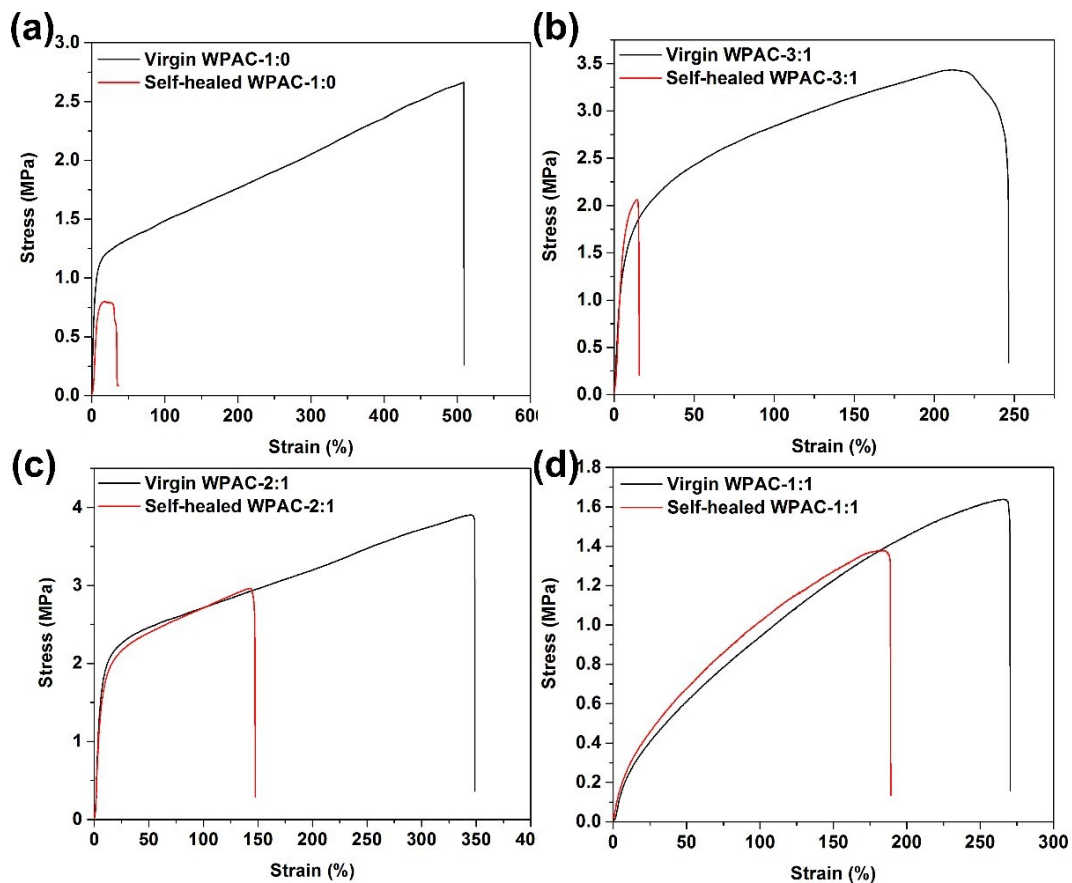


Fig. S5 (a) - (d) Stress-strain curves of virgin WPACs films and after self-healed WPACs films.

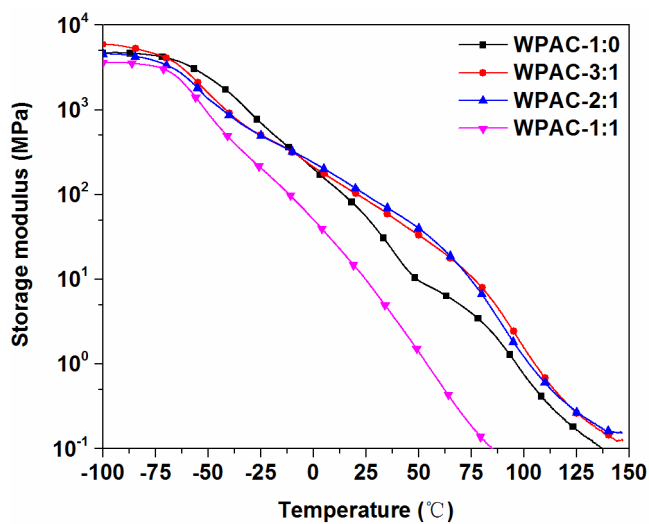
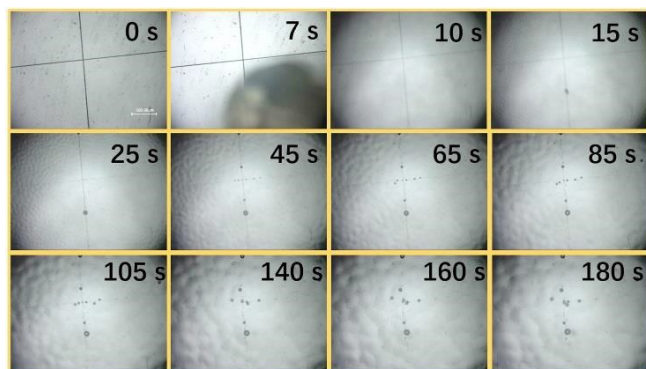
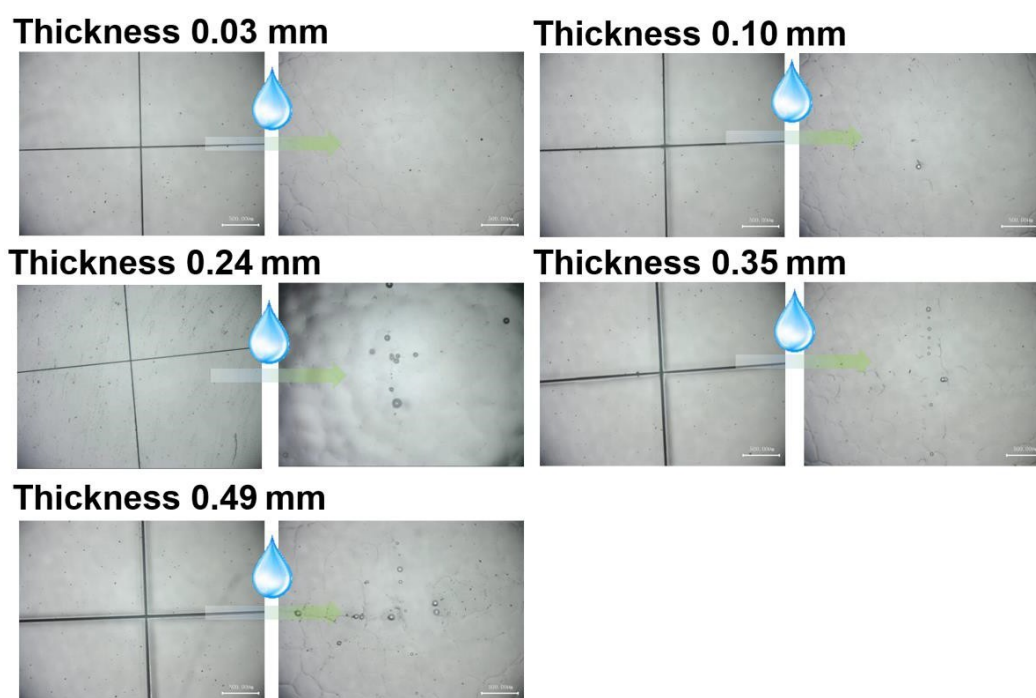


Fig. S6 Storage modulus-temperature curves of WPAC-1:0, WPAC-3:1, WPAC-2:1 and WPAC-1:1 films.



**Fig. S7** Optical microscope images of crisscross scratch on WPAC-2:1 coating before and after water-enabled self-healing. Scale bar: 500  $\mu\text{m}$ .

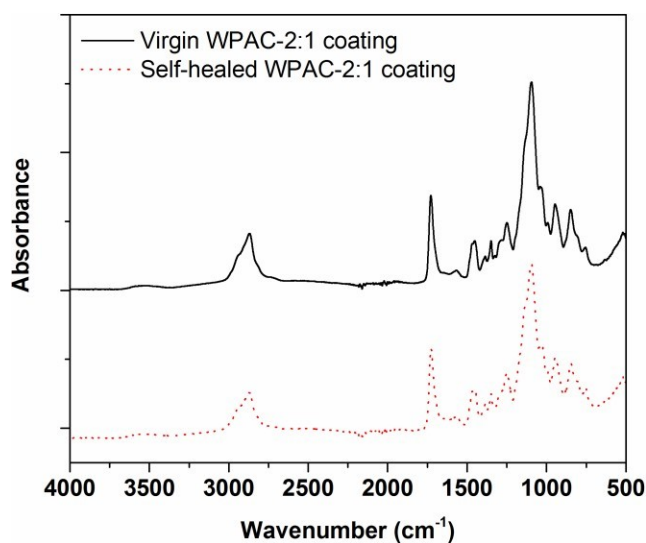


**Fig. S8** Optical microscope images of WPAC-2:1 coating with different thickness before cutting and after self-healing. Scale bar: 500  $\mu\text{m}$ .

WPAC-2:1 coating with different thicknesses were prepared by blade coating the WAPC-2:1 aqueous solution on the substrate via a special bar coater. The thickness of coatings can be tuned by changing the solid content of WAPC-2:1 aqueous solution. The thickness of different WPAC-2:1 coating were 0.03 mm, 0.10 mm, 0.24 mm, 0.35 mm and 0.49 mm (measured by using micrometer) when the solid content of adopted WAPC-2:1 aqueous solution were respectively 10%, 20%, 30%, 40% and 50%. As shown in Fig. S8, the prepared coating still had the good self-healing ability even though the thickness of was as low as 0.03 mm.

**Table S2** Pencil hardness of WPAC-2:1 coating before and after multiple self-healing processes.

Samples	Original	First self-healed	Third self-healed	Fifth self-healed
Pencil hardness	2B	2B	2B	2B

**Fig. S9** FTIR spectra of virgin WPAC-2:1 coating and self-healed WPAC-2:1 coating.**Table S3** Weight changes of WAPCs coatings after multiple cut/self-healing cycles.

Sample	Weight <sup>a</sup> (g)	Weight <sup>b</sup> (g)	Weight loss ratio (%)
WPAC-1:0	0.6154	0.5833	5.216
WPAC-3:1	0.5833	0.5649	3.152
WPAC-2:1	0.6572	0.6238	5.089
WPAC-1:1	0.5204	0.4824	7.302

<sup>a</sup> For the pristine WAPCs coatings. <sup>b</sup> For the dried WAPCs coatings after ten times cut/self-healing cycles.

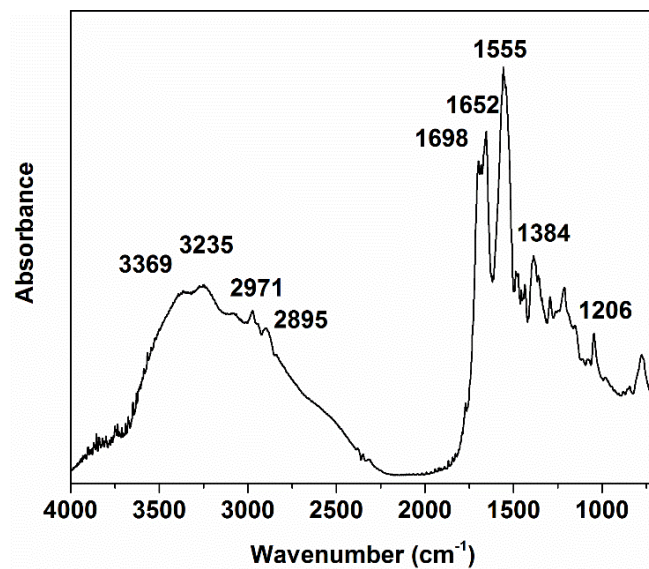


**Fig. S10** FTIR curves of CQs.

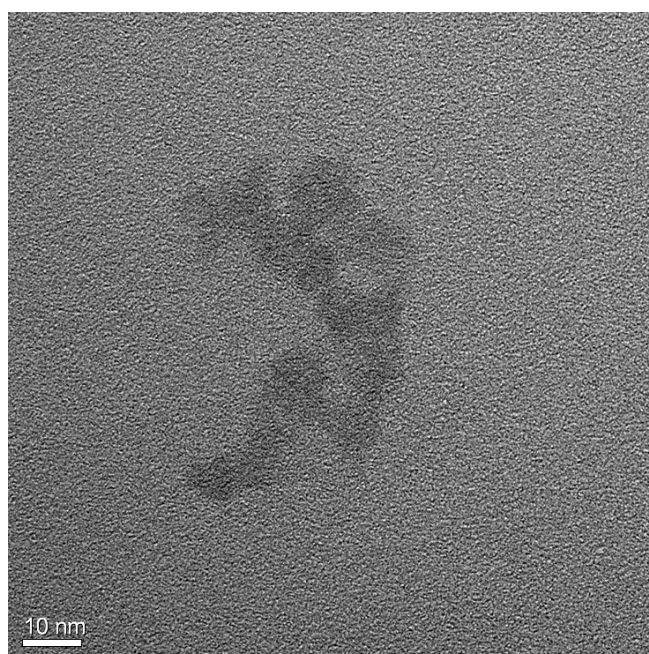


**Fig. S11** TEM images of the prepared CQs.

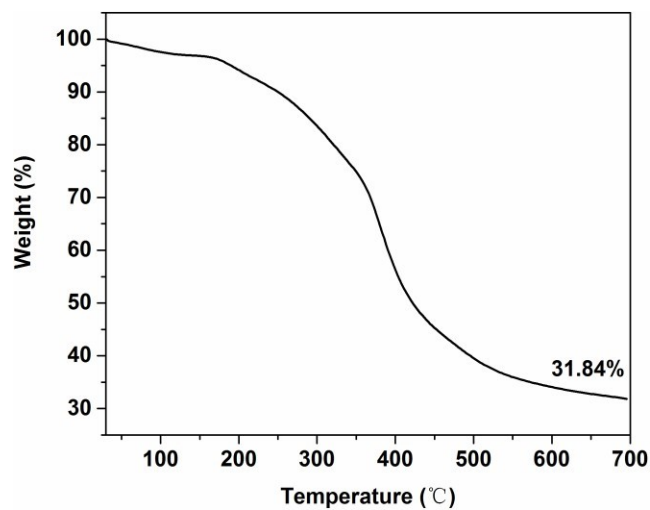


**Fig. S12** TG curves of CQs.

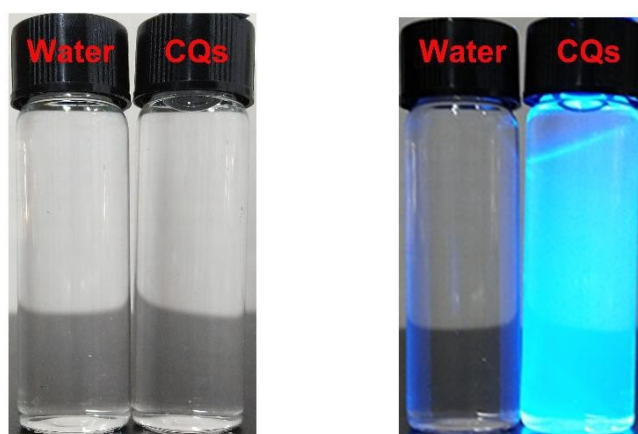


**Fig. S13** Photographs of water and CQs aqueous solution under natural (left) and UV (right) light.

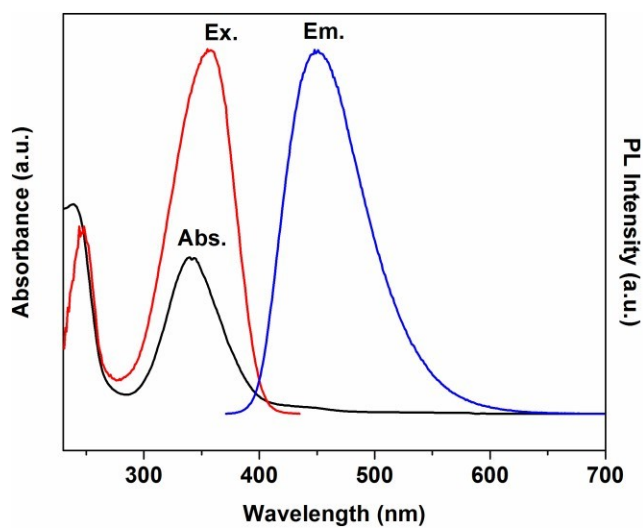


**Fig. S14** UV-vis absorption spectra, the maximum PL excitation and emission spectra of CQs aqueous solution

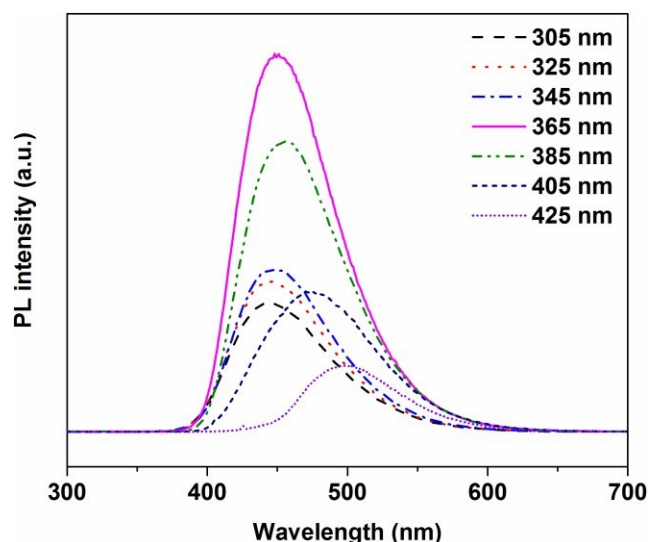


**Fig. S15** PL emission spectra of CQs aqueous solution at different excitation wavelengths.

Carbon quantum dot (CQs) was prepared by one-step hydrothermal method.<sup>30</sup> FTIR spectrum of CQs in Fig. S6 indicate the existence of –OH groups (3369  $\text{cm}^{-1}$ ), –NH groups (3235  $\text{cm}^{-1}$  and 1555  $\text{cm}^{-1}$ ), C=O groups (1698  $\text{cm}^{-1}$ ), C=N bonds (1652  $\text{cm}^{-1}$ ), methyl and methylene groups (2971  $\text{cm}^{-1}$  and 2895  $\text{cm}^{-1}$ ) on CQs surface. TEM image in Fig. S7 shows that the prepared CQs are uniformly spherical nanoparticles with the diameters ranging from 5 nm to 10 nm. Moreover, the CQs displays a good thermal stability with the carbon residue up to 30% (Fig. S8). As expected, the CQs aqueous solution is transparent under natural light and exhibits strong blue PL under 365 nm UV excitation (Fig. S9). To further study the PL properties, UV – vis absorption and PL spectra of CQs aqueous solutions were recorded. In Fig. S10, the peak centered at 344 nm in UV – vis spectrum is ascribed to the  $n \rightarrow \pi^*$  transition. PL excitation and emission spectra in Fig. S11 shows that the maximum excitation wavelength ( $\lambda_{\text{ex}}$ ) and maximum emission wavelength ( $\lambda_{\text{em}}$ ) of CQs are 358 nm and 450 nm, respectively. Meanwhile, the prepared CQs display an excitation-dependent PL behavior, which is similar to many previous reported CQs.

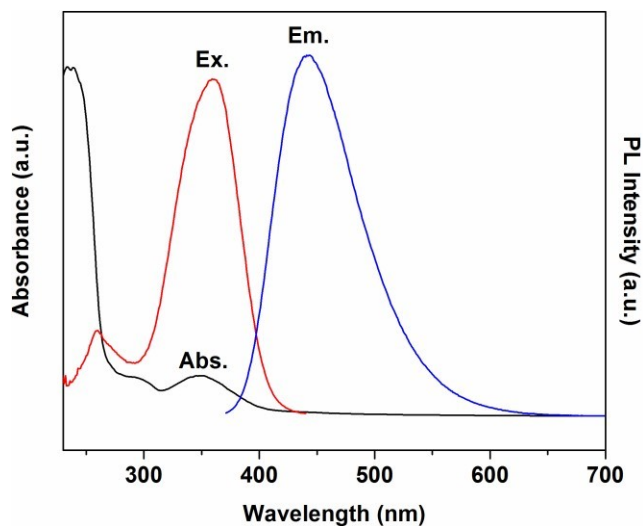


**Fig. S16** UV-vis absorption spectra, the maximum PL excitation and emission spectra of WPAC-2:1/CQs coating (CQs content is 0.5%).

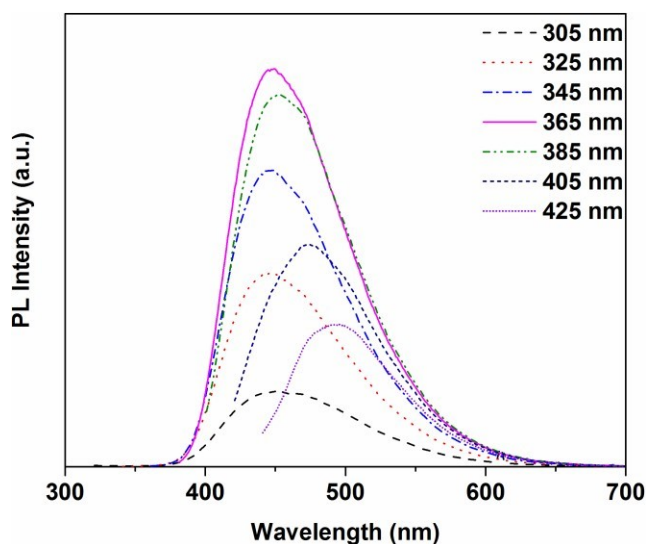


**Fig. S17** PL emission spectra of WPAC-2:1/CQs coating at different excitation wavelengths (CQs content is 0.5%).

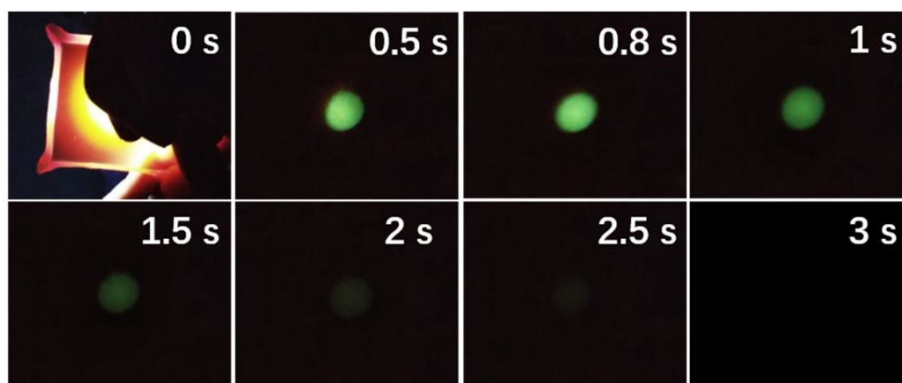


**Fig. S18** Photographs of WPAC-2:1/CQs film under UV light, and right after UV light has been turned off for different time (CQs content is 0.5%).